NHSEMH - 2023
2nd National Conference on New Horizons in Science, Engineering, Management and Humanities
International Journal of Scientific Research in Science and Technology
Print ISSN: 2395-6011 | Online ISSN: 2395-602X (www.ijsrst.com)

Fatigue Strength Experimental Testing of a Cast Aluminium Alloy

Sunil Kumar Ojha*[1], Dhruv Kumar*[1]
[1]Assistant Professor, Department of Mechanical Engineering, IIMT College of Engineering Greater Noida, Uttar Pradesh, India

ABSTRACT

Fatigue strength of a type A319 cast aluminum alloy was studied by means of fully reversible tension–compression tests conducted at room temperature and at 130 °C; the specimens used in this study came from samples cut from the bulkheads of V-8 type engine blocks. Testing was carried out in a servo-hydraulic machine. The specimens were tested to fracture or up to 107 cycles. Analyses of the fatigue tests yield to a strength of 99.4 and 90.3 MPa at 107 cycles for the tests at room temperature and at 130 °C. The size and nature of the defects that originated the failure were determined by scanning electron microscopy. It was found that fatigue cracks originated in pores; single cracks were observed to occur in samples tested below a nominal reversible stress of 120 MPa; multiple cracks were observed in samples stressed above this value.

Keywords: Fatigue Strength, Failure, Electron Microscopy, Fatigue Cracks.

I. INTRODUCTION

keep The resistance to fatigue of cast aluminium alloys is affected by defects that are related directly to casting; among the defects that exert the higher influence in fatigue are pores, either due to shrink- age or gas evolution, intermetallic inclusions and precipitated par- ticles, as cracks nucleate on the most prominent defects and grow following paths in which smaller defects are concentrated [1–16]. The distribution of these defects is modified by the rate at which the casting solidifies; as smaller sizes and finer distribution are enhanced when the time available for growing is reduced [17,18]. It is normal practice to assess microstructural refining by means of the secondary dendrite arm spacing, DAS, which is related to the heat transfer rate occurring during solidification [19–23]. Most studies on fatigue of cast aluminium alloys have been carried out on Al–Si–Mg alloys, due to their wide use in automotive industry [1–6] and such studies can be used as a basis to under- stand the behavior of Al–Si–Cu alloys. It is suggested that cracks nucleated on large defects propagate through the material along sites that contain a high concentration of smaller defects [1,9,12,13].

Silicon is added to aluminium alloys to enhance fluidity and in- crease their strength, so it is expected to also enhance the resistance to high cycle fatigue, but, as the amount of silicon approaches the eutectic composition, this effect can be reversed as silicon platelets act as nucleation sites for fatigue cracks [9,10]. Cu and Mg are added to Al–Si alloys to increase the mechanical properties by heat treating and they affect fatigue due to the tendency for the

cracks to propagate along the interface of the precipitates [1,9,12,13]. Pieces such as engine blocks and cylinder heads are subjected to thermal fatigue due to the changes in temperature caused by turning on and off the engine and by their operation at high temperatures [2,7]. The aim of this work is to present the results of the studies carried out to evaluate the fatigue life of a cast aluminium alloy used in the manufacture of engine blocks. Thework was conducted on samples heat-treated to T7 condition that were cut from the bulk-heads of engine blocks.

II. EXPERIMANTAL PROCEDURE

A series of samples were cut from the bulkheads of V-8 engine blocks that were cast by low pressure [17,18]. The microstructure of this portion of the engine block is refined by a grey iron insert, which enhances the solidification rate, and allows for the mechanical properties required to withstand the stresses caused by the rotating crankshaft. Fig. 1 shows the position of the bulkhead within a V-8 engine block. The reduction of the secondary dendrite arm spacing, as measured on several bulkheads, that is promoted by the use of the grey iron insert. The position from which the specimens subjected to fatigue were machined isshown in the diagram. The DAS ranges in this region within the 20–30 lm interval.

The engine blocks from which the samples were obtained were cast from two different melts. Samples from the first one, identified as A, were tested at room temperature (22 °C), the samples from the second batch, B, were tested at 130 °C. The chemical composition of both melts is shown in Table 1. The samples were heat-trea- ted to a T7 condition (solubilization at 495 °C for 7 h, immersion in water at 90 °C and aging at 240 °C for 4 h). The specimens were machined to an hour-glass shape with a reduced diameter of 6.0 ± 0.05 mm at their centre, following a radius of curvature of 48.0 ± 0.25 mm from cylindrical bars of 15.0 ± 0.02 mm. Tensile test were carried out at room temperature following the ASTM standards B-557 [26] and E-8 [27] in samples cut and machined from additional bulkheads; these specimens were of 12.7 mm in diameter by 62.7 mm in gauge length. Fatigue tests were fully reversible.

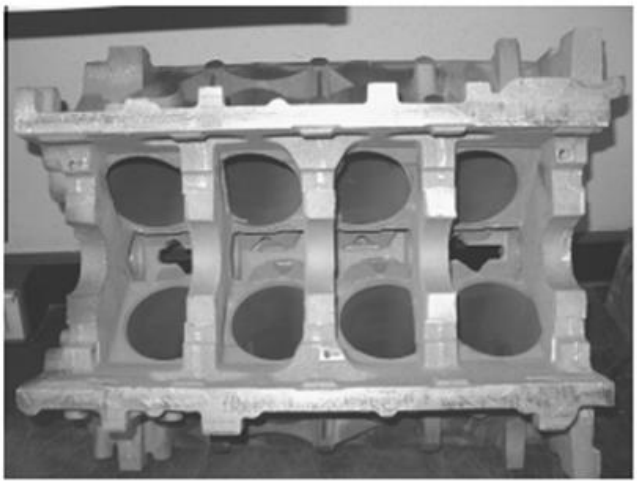

Figure -1,Position of the bulkhead within a V-8 engine block

The value of stress used along the text will be that of rmx.2.The frequency used in all tests was of 75 kHz an all were con- ducted either at room temperature (22 °C) or at 130 °C, the latter was accomplished with the aid of a small heating chamber; tensile tests were carried out only at room temperature. Fatigue testing followed a reduced staircase schedule [28]. The specimens were tested up to failure or until a number of 107 cycles was achieved; the reversible stress was computed from the original cross-section of the specimen. The trials at room temperature started with a stress (Dr/2) of 160 MPa, the stress level was then reduced by 10 MPa in the following test upon failure; this procedure was modified to the reduction or increase in stress in 5 MPa steps once the first sample withstand 107 cycles. The trials at 130 °C started with reversible stress amplitude of 90 MPa and were followed by reducing or increasing the stress in 5 MPa steps. The samples that resisted 107 cycles were then subjected to fatigue with an increase in stress of 10% to promote their failure and measure the size of the defect that caused it.Failure and metallographic analyses were conducted on fractured specimens

byscanning electron microscopy (SEM) and optical microscopy (OM). The size and type of defect that originated the fatigue crack was recorded, as well as the length and area of propagation of the crack. The samples were then cut along their axis to measure DAS and porosity close to the reduced section.

III. RESULT

The microstructure of the as-cast specimens is shown in Fig. 2a, which is typical of a modified hipoeutectic Al–Si alloy. Proeutectic aluminium dendrites are nucleated and grow at a speed that de- pends on the heat transfer rate; the separation between the secondary dendrite arms is used to rate solidification [19–23]. Fig. 2b and c shows the microstructures of samples treated to the T7 condition thatwere subjected to fatigue either at room temperature, Fig. 2b, or at 130 °C, Fig. 2c. It can be seen that heat treating contributes to rounding of the silicon platelets of the eutectic aggregate [19].

The results from the tension tests carried out at room temperature on samples in the ascast the quality index (Q) is calculated by [20,21].

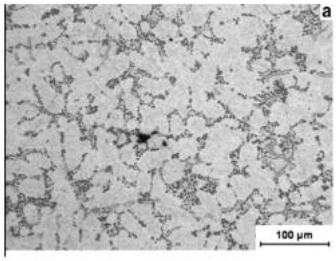

Figure-2 (a)

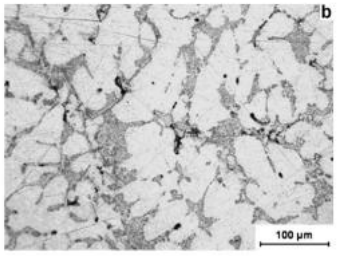

Figure-2(b)

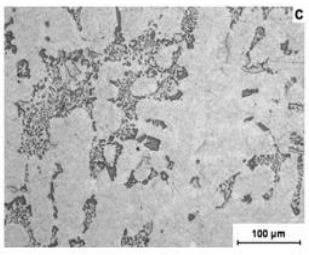

Figure-2 (c)

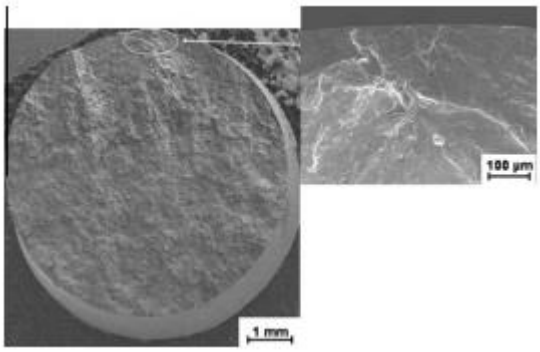

Figure-3 (a)

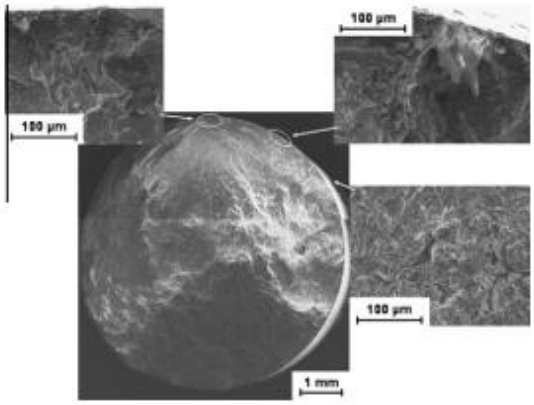

Figure-3 (b)

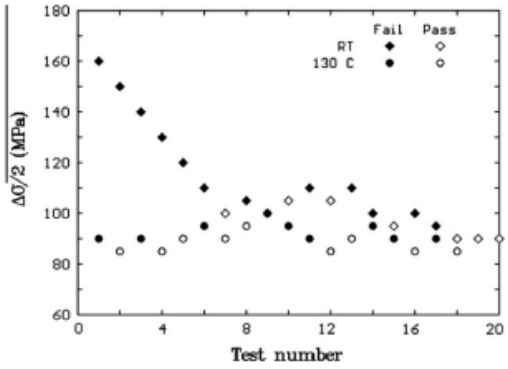

Figure -4 (a)

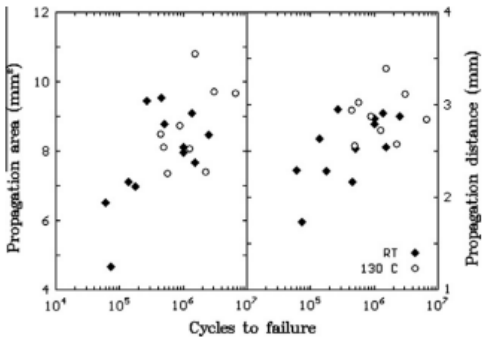

Figure -4(b)

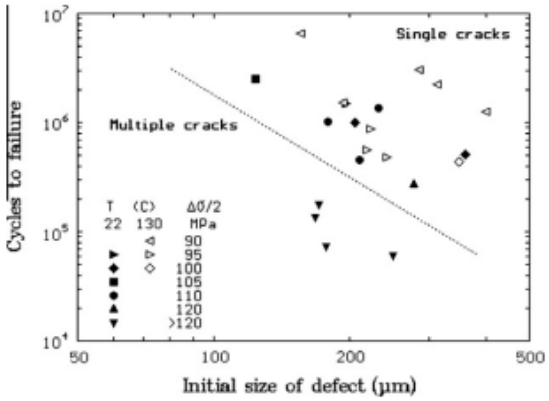

Figure-4 (c)

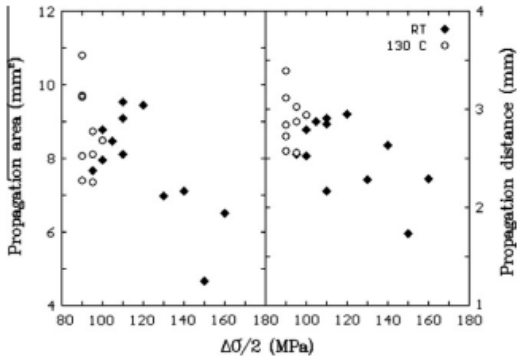

Figure-4 (d)

where ru and Dl are the ultimate tensile strength and the elongation to fracture.Fig. 4 shows the staircase schedules for the tests conducted at both temperatures, the specimens that failed before reaching the 107 cycles, or that resisted this number are identified by either full or empty symbols; the staircases started at a stress of 160 and 90 MPa respectively for 22 and 130 °C; the stress for the following.

sample was either reduced or increased depending on the failure or survival of the specimen.

The fracture surface of the samples was observed by SEM to detect the origin of the failure. It was found that some specimens developed a single crack, Fig. 5, which was able to propagate and cause the failure of the specimen, whereas failure in other specimens occurred by the propagation of multiple cracks, Fig. 6. It was found that the specimens that failed by the propagation of single cracks were stressed below ±120 MPa. SEM was used to identify the defects that originated the cracks and measure the propagation distance and the area covered by the cracks. Fig. 7 shows the fracture area of a sample tested at room temperature with ±105 MPa.

Fig. 8 shows the number of cycles to failure of the specimens as a function of the size of the defect that originated the crack. Figs. 9 and 10 show that the distance and area that the cracks were able toto the stress to which the samples were subjected, Fig. 10. Figs. 9 and 10 can be interpreted in terms of the toughness of the material, as shorter cracks will be able to promote failure at higher stresses.

IV. DISCUSSION

Fig. 8 plots the number of cycles that the specimens resisted as a function of the size of the defect that caused the failure (pores in all cases). The tendency of the data is for a reduction in the number of cycles to failure as either the stress or the size of the pore increase; a line is drawn to discriminate between the samples stressed above or below ±120 MPa, as the samples tested above this value, showed multiple crack propagation, see Fig. 6. Previous research [6,8] have shown a correlation between the size of the biggest pore with the number of cycles to failure in Al–Si–Mg alloys; the difference between the previous works and the present is that in the former ones the size of the pore was varied by changing the solidification rate, whereas in this work the solidification rate was kept within a narrow range, as can be verified by the similarity in DAS in all specimens tested. Of more importance will be the distance and area of the crack that propagate in fatigue, as will be discussed later on.

Fig. 11 shows the S–N curves of the experimental alloy at both testing temperatures. The fatigue limits of 99.4 and 90.3 MParespectively for 22 and 130 °C were calculated from the reduced staircases. Data points from a similar alloy with 23lm DAS tested at lower frequency (20 and 40 kHz) [21] are added for comparison.

V. CONCLUSIONS

Results from the fatigue tests indicate that the fatigue limit in the material is of 99.4 and 90.3 MPa when testing at 22 or 130 °C, which represent a 10% decrease in the fatigue limit at the higher temperature. Measurement of the distance and area that the cracks propagate before failure allowed for computing the threshold for the stress intensity factor these values werethen used to compute the average critical stress (rcr) that resultedin 99 and 90 MPa respectively for the material tested at 22 and 130 °C.

Fractographic analyses carried out on the samples show that the cracks nucleate on existing pores, which were in all cases close to the surface of the specimen. It was found that failure occurred by the propagation of single cracks when the samples were strained below 120 MPa; propagation of multiple cracks were found to occur when testing at higher stresses.

It was found a tendency for a reduction in the number of cycles to failure with the increase in the size of the defect on which the fatigue crack was nucleated.

VI. REFERENCES

[1]. Wickberg A, Gustafsson G, Larsson LE. Microstructural effects on the fatigue properties of a cast Al7SiMg alloy (A356), 1984 SAE techn paper 840121, SAE, Warrendale; 1984.

[2]. Culver LE, Balthazar JC, Radon JC. Temperature effects on the fatigue behaviour of an aluminium–silicon alloy. Trans Can Soc Mech Eng 1984;8:150–6.

[3]. Couper MJ, Neeson AE, Griffiths JR. Casting defects and the fatigue behaviour of an aluminium casting alloy. Fatigue Fract Eng Mater Struct 1990;13:213–27.

[4]. Skallerud B, Iveland T, Harkegard G. Fatigue life assessment of aluminum alloys with casting defects. Eng Fract Mech 1993;44:857–74.

[5]. Stanzl-Tschegg SE, Mayer HR, Tschegg EK, Beste A. In-service loading of AlSi11 aluminium cast alloy in the very high cycle regime.IntJFatigue1993;15:311–6.

[6]. Major JF. Porosity control and fatigue behavior in A356–T61 aluminum alloy. Trans AFS 1998;105:901–6.

[7]. Maier HJ, Smith TJ, Sehitoglu H. Modeling high-temperature fatigue behaviorof cast 319-type aluminium alloys. VDI Berichte, no. 1472; 1999. p. 409–22.

[8]. Zhang B, Poirier DR, Chen W. High cycle fatigue crack initiation site distribution in A356.2. In: DasS, editor.Automotivealloys. Warrendale: TMS; 2000. p. 315–24.

[9]. Seniw ME, Conley JG, Fine ME. The effect of microscopic inclusion locations and silicon segregation on fatigue lifetimes of aluminum alloy A356 castings. Mater Sci Eng A 2000;285:43–8.

[10]. Gall K, Yang N, Horstemeyer M, McDowell DL, Fan J. The influence of modified intermetallics and Si particles on fatigue crack paths in a cast A356 Al alloy. Fatigue Fract Eng Mater Struct 2000;23:159–72.

[11]. Chen W, Zhang B, Poirier DR. Effect of solidification cooling rate on the fatigue life of A356.2–T6 cast aluminium alloy. Fatigue Fract Eng Mater Struct 2000;23:417–23.

[12]. Boileau JM, Allison JE. The effect of solidification time and heat treatment on the fatigue properties of a cast 319 aluminum alloy. Metall Mater Trans A 2003;34A:1807–20.

[13]. Chan KS, Jones P, Wang Q. Fatigue crack growth and fracture paths in sand cast B319 and A356 aluminum alloys. Mater Sci Eng A 2003;341:18–34.

[14]. Wang QG, Davidson CJ, Griffith JR, Crepeau PN. Oxide films, pores and fatigue lives of cast aluminum alloys. Metall Mater Trans B 2006;36B:887–95.

[15].Surappa MK, Blank E, Jaquet JC. Effect of macro-porosity on the strength and ductility of cast Al–7Si–0.3Mg alloy. Scripta Metall 1986;20:1281–6.

[16].Kobayashi T. Strength and fracture of aluminum alloys. Mater Sci Eng A 2000;280:8–16.

[17].Biloni H, Boettinger WJ. Solidification. In: Cahn RW, Haasen P, editors. Physical metallurgy, 4th ed. Amsterdam: North Holland; 1996. p. 669–842.

[18].Campbell J. Castings. Oxford: Butterworth-Heinemann; 2000.

[19].Spear RE, Gardner GR. Dendrite cell size. ASF Trans 1963;71:209–15.[20]Granger DA, Ting E. Structures in directionally solidified aluminum foundry alloy A356. In: Stefanescu DM, Abbaschian GJ, Bayuzick RJ, editors. Solidification processing of eutectic alloys. Warrendale: TMS; 1988. p. 105–20.

[20].Jaquet JC, Hotz W. Quantitative description of the microstructures of aluminum foundry alloys. Cast Metals 1992;4:200–25.